Journal of Chromatography B, 875 (2008) 81–92

Contents lists available at ScienceDirect

Journal of Chromatography B

journal homepage: www.elsevier.com/locate/chromb

Effect of the solute molecular structure on its enantioresolution on cellulose tris(3,5-dimethylphenylcarbamate)☆

Rahul B. Kasat, Siao Yee Wee, Ji Xian Loh, Nien-Hwa Linda Wang, Elias I. Franses*

School of Chemical Engineering, Purdue University, 480 Stadium Mall Drive, West Lafayette, IN 47907-2100, USA

ARTICLE INFO

Article history:
Received 17 April 2008
Accepted 17 June 2008
Available online 1 July 2008

Keywords:
Polysaccharide
Ephedrine
Chiral discrimination
Chiralcel OD
Hydrogen bonding
π–π
Steric interactions

ABSTRACT

The effects of the molecular structures for 13 structurally similar chiral solutes on their HPLC retention and enantioresolutions on a commercially important polysaccharide-based chiral stationary phase, cellulose tris(3,5-dimethylphenylcarbamate) (CDMPC) are studied. Among these 13 solutes, only methyl ephedrine (MEph) shows significant enantioresolution. The retention factors of these chiral solutes vary significantly from 0.7 to 3.2 in *n*-hexane/2-propanol (90/10, v/v) at 298 K. The retention factors of some simpler non-chiral solutes having similar but fewer functional groups than their chiral counterparts are also studied under the same conditions and are compared to those of the chiral solutes. The H-bonding interactions between the functional groups of the solute and the C═O and NH functional groups of the polymer are probed with attenuated total reflection-infrared spectroscopy (ATR-IR) for the polymer, for binary sorbent–solute systems. The CDMPC IR amide band wavenumbers change significantly, indicating H-bonding interactions of the polymer C═O and NH groups with the solutes. The elution orders predicted for the enantiomers of these chiral solutes using molecular dynamics (MD) simulations of the polymer–solute binary systems are consistent with the HPLC results. The CDMPC cavity nano-structure and the potential interactions with chiral solutes are proposed based on HPLC data, IR data, and the simulations. The results are consistent with the three-point attachment model and support the hypothesis that significant enantioresolution requires at least three different synergistic interactions which can be a combination of steric hindrance, H-bonding, or π–π interactions.

1. Introduction

Several highly selective cellulose-based chiral stationary phases (CSPs) developed by Okamoto and coworkers are widely used in chiral separations [1]. One of the commonly used CSPs in this class is cellulose tris(3,5-dimethylphenylcarbamate) (CDMPC) (Fig. 1). A study to separate 510 racemates on CDMPC resulted in complete resolution of 229 racemates and partial resolution of 86 racemates (total 62%), indicating the importance of this CSP in chiral chromatography [1,2]. The hydroxyl groups at 2, 3 and 6 positions in each glucose unit of cellulose are substituted with 3,5-dimethylphenylcarbamate residues. The substituted polymer has a backbone with a conformation of left-handed 3-fold helix [3–6]. CDMPC has been used in the separations of aromatic hydrocarbons, cyano or carbonyl compounds, amines, alcohols, amino acid derivatives, β-blockers, etc. [7–9]. The chiral recognition mechanism of this CSP is not yet completely elucidated.

Selditz et al. measured the retention factors and enantioresolutions of 32 racemic 2-amidotetralins in order to provide the insight into the chiral recognition mechanism of CDMPC [10]. They inferred from their high performance liquid chromatography (HPLC) data that hydrogen bonding (H-bonding), phenyl–phenyl (π–π) interactions, and steric factors play important roles in the separations of these solutes. Aboul-Enein et al. studied the separations of several aryloxyaminopropan-2-ol derivatives in HPLC for CDMPC [11]. They concluded that the sorbent–solute π–π interactions are crucial for CDMPC chiral discrimination. Svensson et al. also used HPLC to study the separations of 16 racemic amino alcohols using CDMPC. They investigated the influence of the solute structure (e.g. the distance between the chiral center and the solute nitrogen atom, and the type and position of substituents in the solute phenyl ring) on its enantioresolution [12]. Fukui et al. used HPLC to compare the separations of several alcohols with CDMPC in various polar and non-polar solvents with 2-propanol and benzene as modifiers. They concluded that the π–π interactions between the solute and the polymer phenyl (Ph) groups play an important role in the chiral

☆ This paper is part of the Special Issue 'Enantioseparations', dedicated to W. Lindner, edited by B. Chankvetadze and E. Francotte.

* Corresponding author. Tel.: +1 765 494 4078; fax: +1 765 494 0805.
E-mail address: franses@ecn.purdue.edu (E.I. Franses).

1570-0232/$ – see front matter © 2008 Elsevier B.V. All rights reserved.
doi:10.1016/j.jchromb.2008.06.045

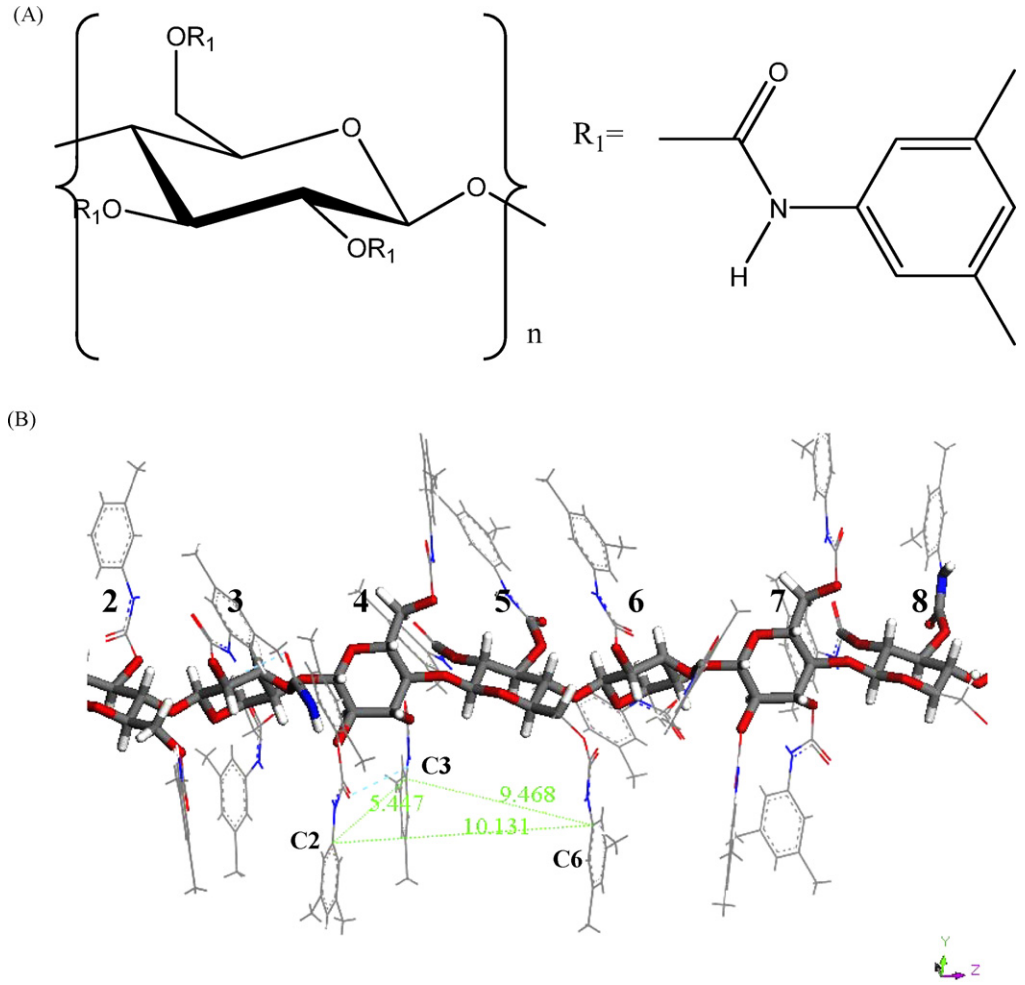

Fig. 1. (A) Molecular structure of cellulose tris(3, 5-dimethylphenylcarbamate) (CDMPC), (B) 3-D structure of CDMPC 9-mer (3 unit cells) generated using Materials Studio. The backbone atoms are shown with ball and stick representation while the side chains are shown with line representation. The monomers are numbered from 1 to 9, and monomers 2–8 are shown. The distances between C2, C3, and C6 side chains give an indication of the cavity dimensions.

recognition of the solutes by CDMPC [13]. These studies only used HPLC data and provided no direct evidence of the specific binding sites of solutes with CDMPC.

Several spectroscopic studies are available for elucidating the polymer structure and its chiral recognition mechanism. Kasat et al. studied the effect of backbone (amylose vs. cellulose) and the side chain on the H-bonding states of the C=O and NH groups in three polymers, CDMPC, amylose tris(3,5-dimethylphenylcarbamate) (ADMPC), and amylose tris((*S*)-α-methylbenzylcarbamate) (ASMBC) [5]. They used attenuated total reflection-infrared spectroscopy (ATR-IR), X-ray diffraction (XRD), ^{13}C cross-polarization/magic angle spinning (CP/MAS), MAS solid state nuclear magnetic resonance (NMR), and density functional theory (DFT) modeling [5] in their study. Recently, Kasat et al. also studied the key interactions of a chiral solute, 2-amino-1-phenyl-1-propanol (PPA), with CDMPC, ADMPC, and ASMBC using HPLC, IR, XRD, and molecular simulations [6]. The elution orders predicted for the PPA enantiomers were consistent with the HPLC results [6]. Chankvetadze et al. compared the infrared (IR) spectra of CDMPC with those of cellulose tris(3,5-dichlorophenylcarbamate) (CDCPC) in the 3000–4000 cm^{-1} spectral region [14]. They related the separation behaviors of these polymers for chiral sulfoxides to the fraction of the polymer's free NH groups [14].

Yamamoto et al. performed computational studies of the interactions between two chiral solutes, *trans*-stilbene oxide and benzoin, and two cellulose-based CSPs, CDMPC and cellulose tris(phenylcarbamate) (CTPC) using three different forcefields [15]. When the enantiomers of chiral solutes were generated in the polymer cavities, significant differences in the interaction energies were observed, suggesting that both the carbamate and the phenyl groups play important roles in the chiral discrimination [15].

Various other cellulose-based CSPs have also been studied in the literature. Okamoto et al. synthesized mono- and disubstituted derivatives of cellulose trisphenylcarbamate, to study the effects of various substituents on trisphenylcarbamate residues using ^{1}H solution state NMR spectra for the NH protons and IR spectra for the NH vibrations [16]. The inductive effects of the substituents and the interactions of a heteroatom with a solute were considered to play important roles on the chiral recognition [16]. Okamoto et al. studied the resolution of some chiral solutes on four different derivatives of cellulose carbamate with different substituents on the side chain Ph groups [17]. The ^{1}H NMR chemical shifts of the NH proton for these polymers were similar, suggesting similar polarities of the carbamate groups. They attributed the differences in the separation behavior of these polymers to the steric hindrance from the substituents on the polymer side chains [17]. Yashima et al. elucidated the chiral discrimination mechanism of cellulose tris(5-fluoro-2-methylphenylcarbamate) for 1,1′-bi-naphthol using HPLC, ^{1}H and ^{13}C solution state NMR, and molecular modeling [4]. They also used spin-lattice relaxation

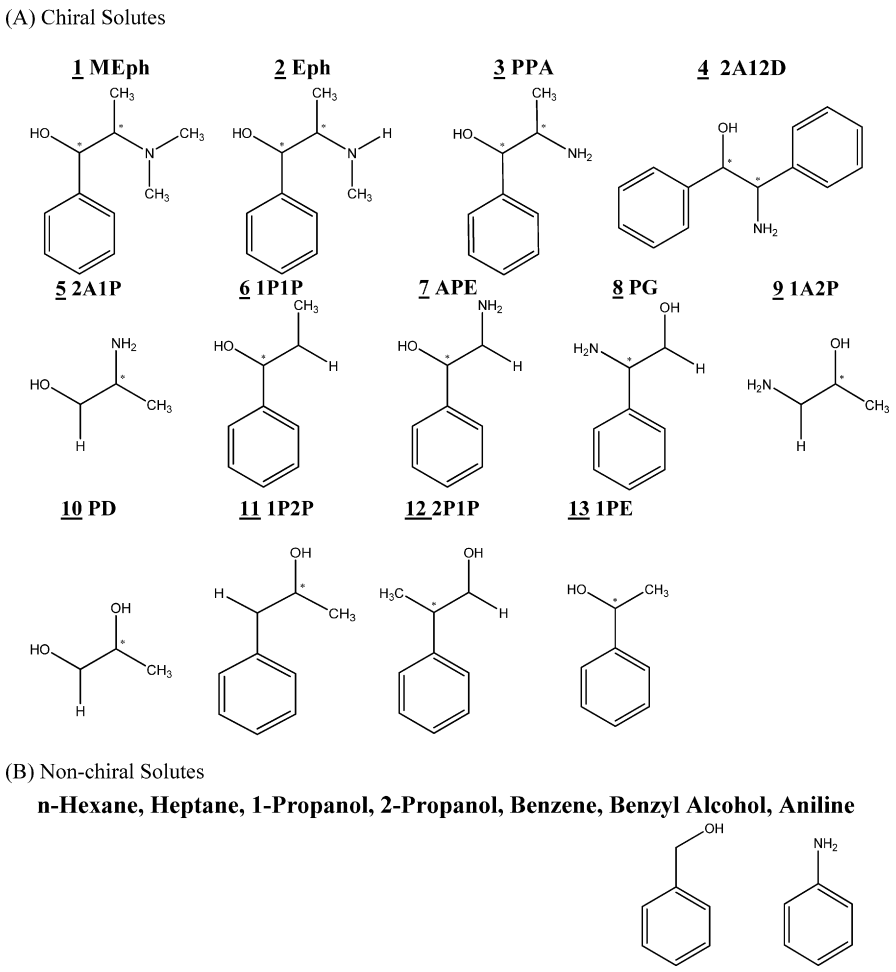

Fig. 2. Molecular structures of (A) 13 chiral, and (B) some non-chiral solutes. The chiral centers are marked with *; see Table 1.

time, ^{1}H NMR titrations, and intermolecular Nuclear Overhauser Enhancements (NOEs), to provide insights into the sorbent–solute binding geometry and dynamics [4]. Sorbent–solute H-bonding, two for one enantiomer vs. one for the other, and π–π interactions were proposed to be the cause for the chiral discrimination. Yashima et al. also related their HPLC separation behavior for different chiral solutes with the changes observed in the solution state ^{1}H NMR chemical shifts of trisphenylcarbamate derivatives of cellulose, amylose, and oligosaccharides [18]. An H-bond between the NH groups of cellulose tris(4-trimethylsilylphenylcarbamate) and the oxygen atom in *trans*-stilbene oxide was proposed [18]. O'Brien et al. studied the chiral discrimination mechanism of cellulose tris(4-methylbenzoate) for a diol analyte using modeling and chromatographic, calorimetric, and spectroscopic data. They attributed the enantioselectivity to differences in the H-bonding interactions of the two enantiomers with the polymer [19]. Chankvetadze et al. obtained the IR and ^{1}H NMR spectra of NH for various cellulose chloromethylphenylcarbamate derivatives. They related the separation behavior of these polymers to the chemical shifts of NH protons [20].

The above studies for CDMPC and related polymers suggested that the side chains surrounding the helical polymer backbones create nano-sized chiral cavities. Different stereospecific interactions, and the enantioresolution, are presumed to result from the incorporation of the enantiomers of a chiral solute in these cavities. The binding sites of these polymers may involve the main polar groups of the carbamate side chains, C=O and NH, which interact with the enantiomers through H-bonding interactions. The Ph groups of the carbamate side chains are also presumed to have π–π interactions with the solutes [1,2].

The main objective of this study is to provide insights in the necessary and sufficient conditions required for the chiral recognition with CDMPC using certain chiral solutes and HPLC, ATR-IR, and MD simulations. In the present study, the HPLC retention factors and enantioresolutions of various structurally similar chiral solutes (Fig. 2), with systematic addition or deletion of certain functional groups, are compared. Unlike previous studies [10–12], in which larger chiral solutes were used, the solutes used in this study are simpler with fewer functional groups. Moreover, comparing these retention factors to those of simpler chiral or non-chiral solutes can help understand the number and the nature of the key functional groups involved in the sorbent–solute interactions. The H-bonding interactions between the polar functional groups of chiral and non-chiral solutes with the polymer functional groups (C=O and NH) are probed using ATR-IR for the sorbent–solute binary systems. MD simulations of some chiral solutes "docked" into a polymer cavity provide further insights into the potential sorbent–solute binding sites and the chiral recognition mechanism of CDMPC. The results indicate that the substantial resolution of enantiomers of MEph is due to three different synergistic interactions, steric hindrance, H-bonding, and π–π. Moreover, a rationale is given why some simple chiral compounds are not resolved in these cavities.

2. Experimental and computational methodologies

2.1. Chemicals

CDMPC-polymer-coated silica beads and semi-preparative Chiralcel OD columns (100 mm long × 10 mm diameter, 20 μm diameter particles) were provided by Chiral Technologies (Exton, PA, USA). HPLC grade 2-propanol, *n*-hexane, and aniline were purchased from Mallinckrodt Chemicals (Phillipsburg, NJ, USA). 1-propanol, tetrahydrofuran (THF), and benzene were purchased from J. T. Baker Co. (Phillipsburg, NJ, USA). Benzyl alcohol was purchased from Fisher Chemicals (Fair Lawn, NJ, USA). 1-Heptanol, 1,3,5-tri-tertbutylbenzene (TTBB), (1*R*,2*S*)-(−)-2-dimethylamino-1-phenylpropanol (methylephedrine or MEph, 99%), (1*S*,2*R*)-(+)-MEph (99%), (1*R*,2*S*)-(+)-2-methylamino-1-phenyl-1-propanol (ephedrine or Eph, 98%), (1*S*,2*R*)-(+)-Eph (98%), (1*R*,2*S*)-(−)-2-amino-1-phenyl-1-propanol (norephedrine or phenylpropanolamine or PPA, 99%), (1*S*,2*R*)-(+)-PPA (98%), (*R*)-(−)-2-amino-1-propanol (2A1P, 99%), (*S*)-(+)-2A1P (97%), (*R*)-(−)-2-amino-2-phenylethanol (α-phenylglycinol or PG, 99%), (*S*)-(+)-PG (99%), (*R*)-(+)-1-phenyl-1-propanol (1P1P, ≥99%), (*S*)-(−)-1P1P (≥99%), (*R*)-(−)-2-amino-1-phenylethanol (APE), (*S*)-(+)-APE, (1*R*,2*S*)-(−)-2-amino-1,2-diphenylethanol (2A12D), (1*S*,2*R*)-(+)-2A12D, (dl)-1-Phenyl-2-propanol (1P2P), (dl)-1-Phenylethanol (1PE), (dl)-2-Phenyl-1-propanol (2P1P), (dl)-1,2-Propanediol (PD), and (dl)-1-Amino-2-propanol (1A2P) were purchased from Sigma–Aldrich (Milwaukee, WI, USA).

2.2. Instrumentation

The HPLC separation was performed using an apparatus consisting of a Waters 515 HPLC pump, a Rheodyne 7725i injection valve, a Waters 996 photodiode array detection (DAD) system, a Waters 2414 refractive index detection (RID) system, and a personal computer (PC) with Waters Millennium software. All chromatography experiments were carried out at 298 K in a Lunaire CE0932-2 environmental chamber (Williamsport, PA, USA). A Nicolet Protégé 460 Fourier transform infrared (FTIR) spectrometer was used to obtain the FTIR spectra. A WS-400A-6NPP-Lite Spin Processor (Laurell Technologies Corporation, PA, USA) was used for making polymer films on Si ATR plates (Wilmad, NJ, USA).

2.3. Sample preparation

The mobile phase used was *n*-hexane/2-propanol (90/10, v/v) at a flow rate of 1 ml/min. This solvent was also used as sample diluent. The elution time, t_{ref}, of TTBB, which is presumed to be practically non-retained, was used to calculate the retention factor, k, of a chiral solute, as $k \equiv (t - t_{ref})/t_{ref}$, and the enantioselectivity, as $S \equiv k_+/k_-$. The elution time of TTBB with Chiralcel OD was 5.5 min.

The polymer (about 0.2 g) was extracted from the commercial-grade polymer-coated-silica beads (1 g) obtained from Chiral Technologies using THF (5 ml). The approximate weight percentage of polymer in the solution is about 4 wt%. The polymer was spin coated on Si-ATR plates at a spinning speed of 500 rpm for 5 min. The films were annealed in an oven for at least 1 h at 80 °C. All IR spectra were taken at a resolution of 2 cm^{-1} using Happ-Genzel apodization and 256 scans. Each enantiomer of a chiral solute, or a racemic mixture, was dissolved in 90/10 (v/v) *n*-hexane/2-propanol. A few drops of each solution were placed on the polymer films deposited on separate ATR plates. The solvent was allowed to evaporate almost completely. IR spectra were taken after 1 h, and also after 24 h, showing no solvent peaks. The IR spectra for the volatile non-chiral solutes were obtained by using excess of pure solutes, and not allowing for significant evaporation to ensure that a large amount of the solute remained in the polymer.

2.4. MD methodology

A 9-mer (3 unit cells) CDMPC polymer rod with 3-fold helix proposed by Steinmeier and Zugenmaier [3] was constructed using the Linked-Atom Least-Squares (LALS) package. The helical fold of this polymer is consistent with that used by Yamamoto et al. in their computational studies [15]. The polymer pitch length used in generating the helical structure was obtained from our previous XRD results [6].

These structures were then energy-minimized using molecular mechanics simulations, which were done by using the Discover module from the Materials Studio Modeling 3.0 software (Accelrys, CA, USA) [21]. Then, the energies of the polymer rods were first minimized using MD simulations at 500 K for 1 ns, with a time step of 1 fs, using an NVT ensemble, and then again at 298 K for 1 ns, to allow the polymer to overcome energy barriers and fully explore the potential energy surface. Consistent-valence forcefield (CVFF) was used in all simulations [22]. The polymer backbone atoms were fixed in their positions during all the simulations, because they were found to have no substantial mobility, as inferred from ^{13}C CP/MAS and MAS solid state NMR [6]. Various conformations of all the chiral and non-chiral solutes were energy minimized using DFT calculations. The details of these calculations were described in our previous studies [5,6,23,24].

Various nano-sized chiral cavities were observed in the predicted CDMPC structure (Fig. 1). These cavities in a unit cell were studied by inserting the enantiomers of MEph. Some of the cavities were too small and could not accommodate either one of the enantiomers of MEph. A cavity of appropriate size was selected and used in the MD simulations of the sorbent–solute interactions. The predicted H-bonding interactions of the solutes with different side chains in the cavity are discussed in Section 3.3. In simulations of the chiral solutes, each enantiomer was placed in the above selected cavity. The initial locations and orientations of these enantiomers were chosen to be consistent with the inferences from the IR results. MD simulations were then performed on these configurations at 298 K for 1 ns.

3. Results and discussion

3.1. Chromatography results

The retention factor of (1*S*,2*R*)MEph on CDMPC is more than twice that of (1*R*,2*S*)MEph, resulting in a resolution of 2.1 for compound **1** (Table 1). Compound **1** has two potential binding groups, OH and phenyl ring (Ph) which can have H-bonding and π–π interactions with the polymer functional groups (see MD results). In addition, the three CH_3 groups can act as sterically hindering groups. To elucidate the contributions of the various functional groups of different solutes to their retention factors and enantioresolutions, 13 structurally similar chiral solutes, MEph (**1**), Eph (**2**), PPA (**3**), 2A12D (**4**), 2A1P (**5**), 1P1P (**6**), APE (**7**), PG (**8**), 1A2P (**9**), PD (**10**), 1P2P (**11**), 2P1P (**12**), and 1PE (**13**) are studied and compared. Their structures are shown in Fig. 2. In order to further elucidate the contributions of the functional groups to the retention factors of chiral solutes, the retention factors of several simple non-chiral solutes are also measured and are discussed first (Table 2).

3.1.1. Retention factors of simple non-chiral solutes

The non-polar heptane interacts little, if at all, with the polymer, resulting in the same elution time as that of void volume marker,

Table 1
Retention factors (k) and enantioselectivities (S) of chiral solutes with Chiralcel OD with n-hexane/2-propanol (90/10, v/v) mobile phase at 298 K

#	Chiral solute	Potential binding groups	Enantiomer	k	S
1	2-Dimethylamino-1-phenylpropanol (Methyl Ephedrine or MEph)	OH, Ph	+MEph (1*S*,2*R*), −MEph (1*R*,2*S*)	1.5, 0.7	2.1
2	2-Methylamino-1-phenyl-1-propanol (Ephedrine or Eph)	OH, NH, Ph	+Eph (1*S*,2*R*), −Eph (1*R*,2*S*)	1.2, 0.9	1.3
3	2-Amino-1-phenyl-1-propanol (Phenylpropanolamine or Norephedrine or PPA)	OH, NH_2, Ph	+PPA (1*S*,2*R*), −PPA (1*R*,2*S*)	2.4, 2.0	1.2
4	2-Amino-1,2-diphenylethanol (2A12D)	OH, NH_2, Ph, Ph	+2A12D (1*S*,2*R*), −2A12D (1*R*,2*S*)	3.1, 3.1	1.0
5	2-Amino-1-propanol (2A1P)	OH, NH_2	+2A1P (2*S*), −2A1P (2*R*)	1.3, 1.3	1.0
6	1-Phenyl-1-propanol (1P1P)	OH, Ph	+1P1P (1*R*) −1P1P (1*S*)	0.9, 0.9	1.0
7	2-Amino-1-phenylethanol (APE)	OH, NH_2, Ph	+APE (1*S*), −APE (1*R*)	3.2, 3.0	1.1
8	2-Amino-2-phenylethanol (α-phenylglycinol or PG)	OH, NH_2, Ph	+PG (2*S*), −PG (2*R*)	2.6, 2.4	1.1
9	(dl) 1-Amino-2-propanol (1A2P)	OH, NH_2	1A2P	1.4	1.0
10	(dl) 1,2-Propanediol (PD)	OH, OH	PD	0.9	1.0
11	(dl) 1-Phenyl-2-propanol (1P2P)	OH, Ph	1P2P	0.9, 0.7	1.3
12	(dl) 2-Phenyl-1-propanol (2P1P)	OH, Ph	2P1P	0.9	1.0
13	(dl) 1-Phenylethanol (1PE)	OH, Ph	1PE	1.2, 1.0	1.2

HPLC conditions: column size, 100 mm × 10 mm i.d.; flow rate, 1.0 ml/min; detector, RI; injection volume, 20 μl.
All retention factors (k) are calculated using the retention time (5.5 min) of TTBB.
(dl): Racemic mixture was used.
$S \equiv k_+/k_-$.

TTBB (see Section 2.3). An addition of an OH group to heptane, i.e. 1-heptanol, results in a higher retention factor (k = 0.4), possibly due to strong sorbent–solute H-bonding interactions of the solute OH groups with the polymer C═O and NH groups. The retention factor of 1-propanol is similar to that of 1-heptanol, suggesting that the chain length plays little role in these alcohols.

The retention factor for benzene (k = 0.2) is lower than that of the alcohols, but higher than that of heptane (Table 2). Benzene is presumed to interact with the polymer Ph groups via π–π interactions, which are stronger than dispersive interactions, but weaker than H-bonding interactions. The π–π configurations can be of four different types, parallel staggered, parallel displaced, herringbone, and T-shaped [25]. The retention factor of benzyl alcohol is 1.8, which is significantly higher than those of benzene (k = 0.2), 1-propanol (k = 0.5), and 1-heptanol (k = 0.4). It appears that benzyl alcohol forms simultaneously strong H-bonds with the polymer C═O or NH functional groups (see Section 3.2.1, IR results) and π–π interactions with the polymer Ph groups. By adding an NH_2 group to benzene, aniline has a large retention factor (k = 4.2). Synergistic H-bonding and π–π interactions between aniline and the polymer functional groups are stronger than those of benzyl alcohol, possibly due to the aniline's unique geometric and electronic features. The DFT calculations for the interactions of benzyl alcohol or aniline with a single CDMPC side chain also support the hypothesis of synergistic H-bonding and T-shaped π–π interactions (see Section 3.3). Okamoto et al. measured the retention times of benzene and monosubstituted benzenes with cellulose tris(phenylcarbamate) to elucidate the affinities of these solutes with the polymer Ph groups. Anisole and nitrobenzene showed higher retention times than benzene, toluene, ethylbenzene, and halogenated benzenes [16].

Overall, the simple non-chiral solutes with polar functional groups can form strong H-bonding interactions with the polymer, resulting in high retention factors. The Ph groups of the solutes can have π–π interactions with the polymer Ph groups and contribute to the retention factors of the solutes. Synergistic H-bonding and π–π interactions are possible reasons for the high retention factors observed for benzyl alcohol and aniline.

Table 2
Retention factors (k) of simple non-chiral solutes with Chiracel OD with n-hexane/2-propanol (90/10, v/v) mobile phase at 298 K

Non-chiral solute	Potential binding groups	k
Heptane	–	0.0
1-Heptanol	OH	0.4
1-Propanol	OH	0.5
Benzene	Ph	0.2
Benzyl alcohol	OH, Ph	1.8
Aniline	NH_2, Ph	4.2

HPLC conditions: column size, 100 mm × 10 mm i.d.; flow rate, 1.0 ml/min; detector, RI; injection volume, 20 μl.

3.1.2. Retention factors and enantioresolutions of chiral solutes

The +MEph enantiomer of compound **1** has k = 1.5, which is slightly lower than that of benzyl alchohol (k = 1.8). This result suggests that the binding groups of +MEph are similar to those of benzyl alcohol and form synergistic H-bonding and π–π interactions (see also MD results). The –MEph enantiomer has k = 0.7, suggesting one of two possible sorbent–solute configurations for –MEph (i) only one strong H-bond, or (ii) weak synergistic H-bond and π–π interactions (see Section 3.3 below). The difference in the sorbent–solute interactions for two enantiomers of MEph is likely due to steric hindrance caused by the –MEph CH_3 groups. The significantly higher retention factor of –MEph compared to benzene (0.7 vs. 0.2) seems to rule out the possibility of only one type of interaction, such as π–π, between the polymer and –MEph.

The retention factor and enantioresolution of compound **3** have been rationalized previously by using ATR-IR and MD [6] and are shown here for reference. In compound **3**, the NH_2 apparently is not hindered sterically by the CH_3 group and can form H-bonds with the polymer C═O or NH groups (see Section 3.2.2, IR results), resulting in a higher retention factor of compound **3** than those of compounds **1** and **2**.

CDMPC has no enantioselectivity for compound **4**, but the retention factor of compound **4** (k = 3.1) is higher than that of compound **3**. Since compound **4** has two Ph groups, compared to one in compound **3**, the higher retention factor for compound **4** can result from additional π–π interactions of the solute Ph groups with the polymer Ph groups. Compared to compound **3**, compounds **5**, **9**, **10** (having no Ph group), and compounds **6**, **11**, and **12** (having no NH_2 group) have significantly lower retention factors and small or no enantioresolutions. This suggests that the NH_2 and Ph functional groups are important for the resolution of the solute. These compounds are expected to have only two sorbent–solute interactions, resulting in no enantioresolutions, as would be expected from the three-point attachment (TPA) model [26–30].

Compound **7** has no CH_3 group unlike compound **3**, and has a significantly higher retention factor than that of compound **3**, with a very small enantioresolution. The higher retention factors are possibly due to the simultaneous interactions of all three functional groups (OH, NH_2, and Ph) with the polymer functional groups for both enantiomers of compound **7**. Removal of a $CHN(CH_3)_2$ group

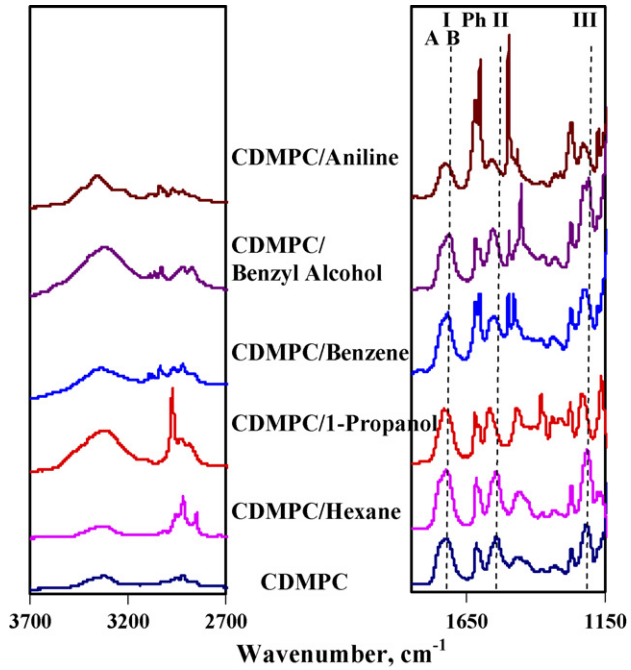

Fig. 3. IR spectra of CDMPC polymer in the dry state and also upon equilibration with simple non-chiral solutes, see Table 3.

in compound **13** compared to compound **1** reduces the size of the steric hindering group and results in lower enantioresolution.

These results show that small changes in the structures of the solutes (compound **1** vs. compound **2** vs. compound **3** vs. compound **4**, and compound **3** vs. compounds **5–8**) can result in significantly different retention factors and enantioresolutions. A minimum of three different and synergistic interactions, H-bonding, π–π, or steric, is required for significant enantioresolution (compound **1**). IR data and simulations are performed to identify the possible binding sites and chiral recognition mechanisms of CDMPC with these solutes.

3.2. ATR-IR results

To elucidate the interactions of non-chiral and chiral solutes with CDMPC polymer with direct spectroscopic evidence, the IR spectra of the CDMPC upon adsorption of different solutes were obtained. It is shown that the bulk structure of the polymer changes significantly upon absorption of the various solutes into the structure. These solutes adsorb into the polymer nanostructured cavities [6]. The spectrum of the CDMPC polymer was analyzed in detail previously using DFT, compared with two other polymers, ADMPC and ASMBC [5], and is shown here for reference. The discussion is focused primarily on the 1800–1500 cm^{-1} region. The amide I and amide II wavenumbers in this region are used as markers of the H-bonding strengths of the polymer C=O and NH groups. Since the solute and polymer bands overlap in the 3200–2900 cm^{-1} region, this region is not examined here (Fig. 3).

The broad peak of the CDMPC polymer in the 1750–1700 cm^{-1} region (Fig. 3 and Table 3) corresponds to the amide I band, which results primarily from 80% C=O stretching and secondarily from 20% NH bending vibrations [31,32]. The amide I band shows a shoulder, and can be thought as the sum of two broad overlapping peaks, which are termed A and B (Table 3) [5,6]. Upon H-bonding a band wavenumber shifts to a lower value for a stretching vibration and to a higher value for a bending vibration [31,32]. Thus, band B is assigned mainly to relatively 'strongly H-bonded' C=O while band A is assigned mainly to relatively 'weakly H-bonded' C=O. Each band, A or B, is also broad, because it arises from a distribution of H-bonding strengths. The amide groups of carbamate residues at C2, C3, and C6 are observed together and consist of groups with inter-chain and intra-chain H-bonds. The amide II band, centered at 1540 cm^{-1}, consists primarily of 60% NH bending and secondarily 40% CN stretching vibrations. The amide III band is a combination of several vibrations (CN stretching, C=O stretching, and NH bending) [31], and is not examined in detail because of its complexity. The Ph (phenyl) band has a major peak at 1614 cm^{-1} and a shoulder at 1603 cm^{-1}, indicating quadrant stretching of the ring carbon–carbon bonds [32].

Table 3
Measured IR peak wavenumbers for different amide and phenyl bands of dry CDMPC polymer alone, and of polymer in the presence of simple non-chiral solutes, see Fig. 3

System	IR wavenumbers (cm^{-1})				
	Amide I		Phenyl peaks	Amide II	Amide III
	A	B			
Dry CDMPC	1744	1725	1614 1603	1540	1213
CDMPC/*n*-Hexane	1742	1725	1614 1603	1540	1213
CDMPC/1-Propanol	1734	1717	1617 1604	1560	1232
CDMPC/Benzene	1741	1719	1617 1603	1553	1224
CDMPC/Benzyl alcohol	1744	1713	1616 1604	1555	1227
CDMPC/Aniline	1735	1725	1618 1601	1557	1230

3.2.1. Effects of adsorption of non-chiral solutes on the IR spectrum of CDMPC polymer

The polymer spectrum remains essentially unchanged upon equilibration of *n*-hexane (Fig. 3 and Table 3). The presence of excess *n*-hexane during the IR experiment is established by the observed CH stretching bands in the 3000–2800 cm^{-1} region. It is inferred that *n*-hexane interacts with the polymer only with weak dispersive forces and no H-bonds, therefore interfering minimally with intra-rod and inter-rod H-bonding interactions in the polymer. This result can explain the significantly lower retention factor for a similarly non-polar compound such as *n*-heptane.

Upon adsorption of excess of 1-propanol (evident from the large H-bonded OH stretching band at around 3300 cm^{-1}), both the wavenumbers and the ratio of the intensities of the peaks A and B of the amide I change slightly. The center of the peak B shifts from 1725 cm^{-1} in the dry polymer to 1717 cm^{-1} and its intensity also increases. Thus, an increase in the population of strongly H-bonded C=O groups is inferred. The centers of the amide II and amide III bands change significantly from 1540 to 1560 cm^{-1} and from 1213 to 1232 cm^{-1}, respectively (Table 3). This indicates that the NH groups in the polymer form stronger H-bonds with 1-propanol than the intra-polymer H-bonds. The Ph peaks show insignificant shifts, and the ratio of the peak intensities remains the same. From these results, we infer that 1-propanol interacts mainly through H-bonding with the polymer C=O and NH groups. Moreover, the change observed in the intensity ratio of the amide I A and B peaks in the CDMPC/1-propanol IR spectrum is different than that in ADMPC/1-propanol [23].

Upon the adsorption of excess benzene (shown in the 3100–3000 cm^{-1} region), the wavenumbers of the amide II and III peaks increase to 1553 and 1224 cm^{-1}, indicating that benzene forms H-bonds with the polymer NH groups, but weaker than with 1-propanol. It is known that benzene electron cloud acts as a weaker H-bond acceptor than alcohols [33,34]. The amide I H-bond distribution does not change significantly, as benzene proton is not a strong H-bond donor [33,34], and thus should form weak H-bonds with C=O groups. The ratio of the intensities of the Ph groups changes only slightly, probably due to weak interactions between

Table 4
Measured IR peak wavenumbers for different amide and phenyl bands of dry CDMPC polymer alone, and of polymer in the presence of chiral solutes, see Fig. 4

System	IR wavenumbers (cm^{-1})				
	Amide I		Phenyl peaks	Amide II	Amide III
	A	B			
Dry CDMPC	1744	1725	1614 1603	1540	1213
CDMPC/+MEph	1746	1721	1615 1601	1545	1216
CDMPC/−MEph	1746	1720	1615 1601	1546	1218
CDMPC/+Eph	1747	1721	1615 1603	1547	1220
CDMPC/−Eph	1745	1720	1615 1603	1547	1222
CDMPC/+PPA	1739	1720	1616 1602	1560	1222
CDMPC/−PPA	1743	1722	1616 1602	1560	1224
CDMPC/2A12D[a]	1747	1719	1615 1603	1550	1220
CDMPC/2A1P[a]	1738	1720	1616 1603	1567	1230
CDMPC/1P1P[a]	1743	1720	1615 1603	1548	1234
CDMPC/APE[a]	1743	1716	1615 1603	1552	1226
CDMPC/PG[a]	1740	1718	1615 1604	1549	1225
CDMPC/PD[b]	1744	1719	1616 1603	1559	1227
CDMPC/1PE[b]	1744	1720	1615 1603	1555	1229

[a] Changes observed in CDMPC polymer spectra upon absorption of both the enantiomers are similar.
[b] Racemic mixture is used.

the polymer Ph groups with those of benzene, consistently with the lower retention factors for benzene.

Upon adsorption of excess benzyl alcohol (having a broad OH stretching band at about 3300 cm^{-1}), the ratio of the intensities of the amide I A and B peaks changes; the intensity of peak B increases, and the center of peak B decreases from 1725 to 1713 cm^{-1}, indicating that there is an increase in the strongly H-bonded C=O groups. The wavenumber of the amide II peak increases, indicating that the polymer NH groups form strong H-bonds with the benzyl alcohol OH groups. Even though the changes observed in the amide bands for 1-propanol and benzyl alcohol are similar, their retention factors are significantly different (Table 2), indicating that benzyl alcohol may have π–π interactions (not detected by IR) with the polymer Ph groups. We infer that benzyl alcohol interacts with the polymer mainly through synergistic H-bonds and π–π interactions.

With the presence of excess aniline (evident at about 1600 cm^{-1}), the amide II and amide III wavenumbers increase to 1557 and 1230 cm^{-1}, respectively, and the changes observed in the amide I band are small, indicating that the polymer NH groups interact strongly with the aniline NH_2 groups.

The changes observed in the CDMPC amide II and III bands wavenumbers upon adsorption of those simple non-chiral solutes are similar to those observed for the ADMPC polymer, which has the same side chains as CDMPC but an amylose backbone [23]. The trends observed for the amide I band of CDMPC are significantly different, however. For ADMPC, the amide I band upon adsorption of one of these solutes splits into two distinct peaks [23], while for CDMPC, the split is insignificant. Hence, the backbone plays a role in modulating the interactions. Some of these compounds are used as mobile phase additives in chromatography separations [1,13,35]. The changes in the polymer's IR spectrum may help explain the effects of the solvents and additives on the chromatographic retention.

3.2.2. *Effects of adsorption of chiral solutes on the IR spectrum of CDMPC polymer*

The IR spectra of the CDMPC upon adsorption of some of the 13 chiral solutes listed in Table 1 are investigated, in order to elucidate the interactions of these solutes with the polymer (Fig. 4 and Table 4). The spectra are for binary polymer–solute systems. The solvent and solute molecules may compete for the binding sites in the polymer in the ternary (or quaternary) systems studied by HPLC.

3.2.2.1. CDMPC/1, 2 and 13 results. The wavenumber of the band B decreases slightly from 1725 to 1721 cm^{-1} and its intensity increases slightly upon adsorption of compound (+)-**1**, indicating a slight increase in the fraction of strongly H-bonded C=O groups. The wavenumber of the center of the amide II band increases from 1540 to 1545 cm^{-1}, indicating that the polymer NH groups form slightly stronger H-bonds with compound (+)-**1** than the intra-polymer H-bonds. The increase in the amide III band wavenumber (1213 to 1216 cm^{-1}, not shown in Fig. 4) supports these inferences. There are also small but reproducible shifts, ~1 cm^{-1}, in the wavenumber of the polymer 1615 cm^{-1} Ph group, suggesting some interactions of the Ph groups with compound (+)-**1**. (The significant increase in the Ph peak intensity at 1601 cm^{-1} is due to an overlap of the IR band of compound **1** with the polymer Ph band.) It is inferred that the changes in the H-bond distribution intensity and the wavenumber of the polymer C=O groups (amide I) and the changes in the wavenumbers of the amide II and III bands are due to the incorporation (adsorption) of compound (+)-**1** in the polymer bulk structure and H-bonding interactions of compound **1** OH groups with polymer C=O, NH, or both groups. With the adsorption of compound (−)-**1** by the polymer, similar changes are observed in the polymer spectra.

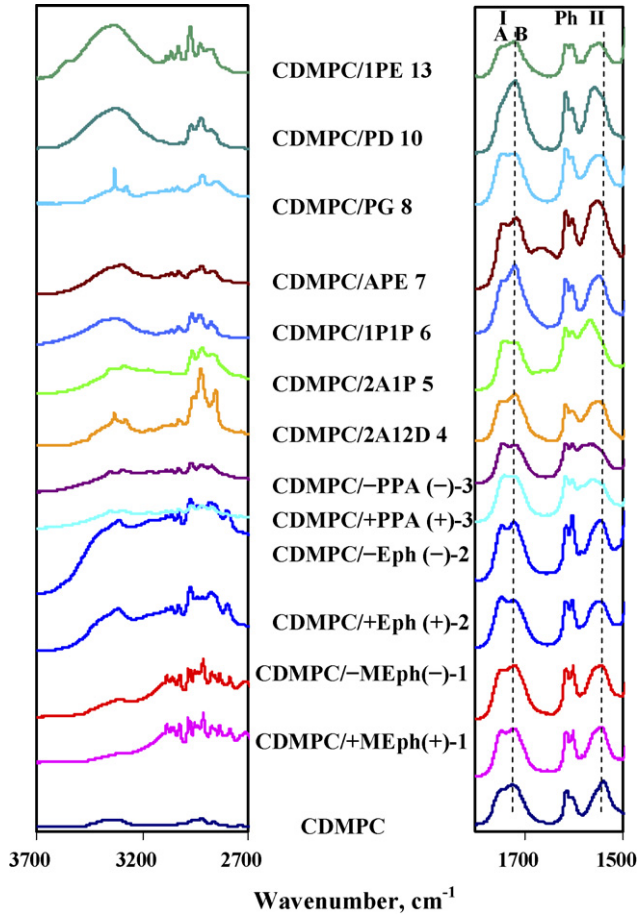

Fig. 4. IR spectra of CDMPC polymer in the dry state and also upon equilibration with chiral solutes, see Table 4. The amide III bands are not shown here. Racemic mixture is used for compounds **10**, and **13**. The changes in the IR spectra for both the enantiomers are similar for compounds **4**, **5**, **7**, and **8**.

Even though the changes observed in the wavenumbers of the polymer amide bands upon adsorption (−)-**1** enantiomer are significantly lower than those observed for 1-propanol, the retention factor of (−)-**1** enantiomer is higher than that of 1-propanol (Tables 1 and 2). This suggests that sorbent–solute π–π interactions also contribute to the retention factor of (−)-**1** enantiomer (see also MD results).

The changes observed in the amide I bands for both enantiomers of compound **2** are similar to those for compound **1**. The amide II and III bands wavenumbers increase due to the H-bonding interactions between the polymer NH groups and compound **2** functional groups.

The changes observed in the amide II and III bands upon adsorption of compound **13** are higher than those in compounds **1** and **2**, indicating that compound **13** can enter more into the polymer cavity because of its smaller steric hindering group, and forms stronger H-bonds, consistent with the HPLC results.

3.2.2.2. CDMPC/3 results. Although the IR spectra of the CDMPC polymer upon adsorption of enantiomers of compound **3** have been reported previously, and compared with those of ADMPC and ASMBC polymers [6], the results are discussed here for comparison. Upon adsorption of each enantiomer of compound **3**, the wavenumbers of the amide II and III bands increase significantly, indicating strong H-bonds between the polymer NH groups and the OH and NH_2 functional groups of compound **3** [6]. Small differences are observed in the wavenumbers and the intensity of the amide I B bands for the two enantiomers. The changes observed in amide I band for compound **3** are higher than those of compounds **1** and **2**. This may be due to the better fit of compound **3** in the polymer cavity, resulting in stronger sorbent–solute H-bonds for compound **3**. The changes in the wavenumbers of the polymer amide groups upon adsorption of **3** are similar to those of 1-propanol and benzyl alcohol and indicate strong H-bonding interactions, which may be the reason for the large observed retention factor of compound **3** in HPLC. Since the retention factors of compound **3** and benzyl alcohol are significantly higher than that of 1-propanol, these solutes may have synergistic H-bonding and π–π interactions with the polymer.

3.2.2.3. CDMPC/4 results. Upon adsorption of either enantiomer of compound **4**, the amide I band B wavenumber decreases and the amide II–III wavenumbers increase, indicating polymer–solute H-bonding interactions. Even though the changes observed in the polymer amide II–III wavenumbers for compound **4** are smaller than those for compound **3**, the retention factor of compound **4** is higher than that of compound **3**, suggesting that the Ph groups of compound **4** play an important role in its retention.

3.2.2.4. CDMPC/5, 9, and 10 results. The wavenumber of the amide II band changes significantly upon adsorption of either enantiomer of compound **5**, compared to all other chiral solutes tested, indicating that compound **5** forms strong H-bonds with the polymer NH groups. Similar changes would be expected to be observed for compound **9** (results not available). The amide II and III wavenumbers change more for compound **5** than for compound **10**, indicating stronger interactions of polymer NH groups with compound **5** NH_2 groups than with the compound **10** OH groups. These results are consistent with the observed retention factors for compounds **5** and **10**.

3.2.2.5. CDMPC/other chiral solutes results. The changes observed in the polymer spectra upon adsorption of compound **6** indicate that the polymer NH and OH groups bind with the compound **6** OH groups. Similar results would be expected for compounds **11** and **12**. Upon adsorption of compound **7**, the wavenumber of the amide I B band decreases significantly, from 1725 to 1716 cm^{-1}, indicating an increase in the number of strongly H-bonded polymer C=O groups. The wavenumbers of the amide II and III bands also increase. For compound **8**, similar spectral changes are observed as those for compound **7**, indicating similar interactions.

Thus, the C=O, and NH groups appear to be the main H-bonding sites of CDMPC with all the chiral and non-chiral solutes tested. The wavenumber and the intensity changes of the amide bands are different for each solute, indicating differences in the strengths of the H-bonding interactions of these solutes with the CDMPC functional groups. The change in the amide II band is a particularly sensitive marker of the strength of interactions of the solute functional groups with the polymer NH groups. This also suggests that some of the NH groups may be buried well inside the chiral cavity. Small solutes (1-propanol, 2A1P, etc.) can access these NH groups easily, while some larger solutes, MEph, Eph, etc., cannot. The small increase in the wavenumbers of the band A of amide I (weakly H-bonded C=O) for larger solutes (MEph, and 2A12D) may be due to the weakening of some of the existing intra-polymer C=O···HN H-bonds upon insertion of these solutes in the chiral cavities.

3.3. MD results

MD simulations were done for the polymer by itself and for the polymer interacting with chiral solutes at 298 K, in the absence of solvent, with the method detailed in Section 2.4. The predicted elution orders for all enantiomer pairs are in agreement with the HPLC experimental results shown in Table 1.

The MD-predicted enantioresolutions for the sorbent–solute systems (no solvent) are significantly higher than those observed in HPLC (with solvent). One reason is that in the present MD simulations only the enthalpic contributions to the retention are considered, and hence only a qualitative agreement may be expected [6]. The following factors would have to be considered in the simulations along with the enthalpic contributions to predict the enantioresolution quantitatively: (a) solvent effects; (b) entropic contributions; and (c) the achiral contributions from the non-discriminating chiral cavities and possibly from any uncoated silica surface. These factors are expected to reduce the observed differences in the interaction energies obtained by the MD calculations [6].

The CDMPC cavity selected in this article for docking studies of chiral solutes is defined as a space between side chains from the C2 and C3 carbons of the monomer 4 in the backbone and the C6 carbon of the monomer 5 (Figs. 1 and 5). The C2 and C6 side chains are at different distances from the C3 side chain. The three side chains are parallel to each other, with C3 slightly shifted compared to C2 and C6. The simulations for the polymer alone predict that there is an intra-polymer H-bond between the NH group of C3 and the C=O group of C2 in this chiral cavity.

The DFT and MD-predicted interactions of benzyl alcohol with the CDMPC side chain and with the polymer cavity, respectively, are shown in Fig. 5. The DFT-predicted energy minimized structures show synergistic H-bonding and π–π interactions between the functional groups of benzyl alcohol with the polymer functional groups. Two different H-bonding sorbent–solute configurations, C=O···HO or NH···OH, were predicted. The sorbent–solute π–π interaction is of T-shaped configuration. The MD results for benzyl alcohol in the polymer cavity also predict synergistic H-bonding and π–π sorbent–solute interactions with slightly different configurations. The OH group of benzyl alcohol interacts with the NH group of C3 via a NH(C3)···OH (benzyl alcohol) H-bond (Fig. 5B and Table 5). The benzyl alcohol Ph groups are predicted to interact with the polymer C2, C3, and C6 Ph groups via herringbone (h)

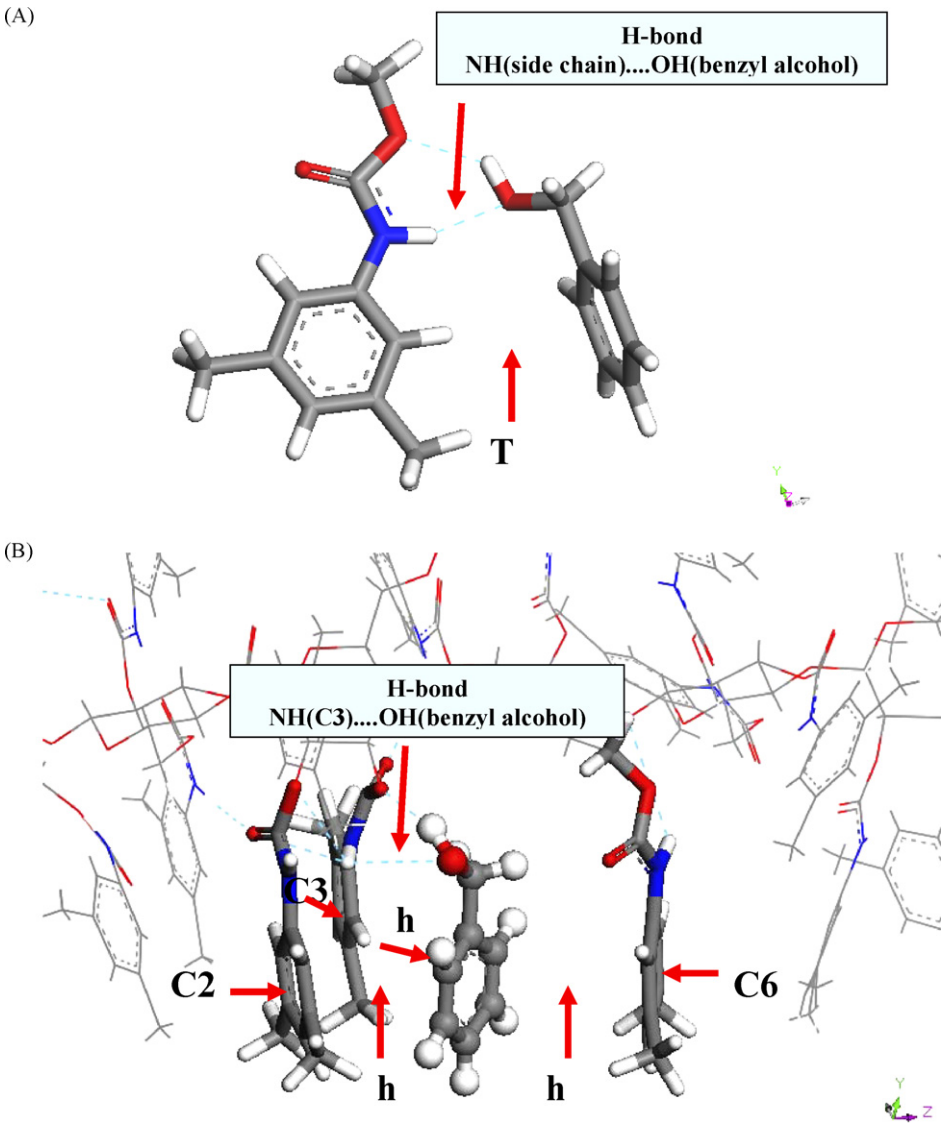

Fig. 5. Energy minimized structures benzyl alcohol complexes with (A) one CDMPC side chain, and (B) CDMPC polymer cavity. The dotted lines indicate H-bonds. The T, and h indicate T-shaped, and herringbone π–π interactions, respectively.

configurations instead of T-shaped configurations, as a result of steric hindrance from the C2 side chain.

The MD-predicted elution order is consistent with the HPLC result for compound **1**. The MD results predict that the OH group of (+)-**1** enantiomer interacts with the NH group of C3 via a NH(C3)···OH((+)-**1**) H-bond (Fig. 6 and Table 5). The Ph groups of (+)-**1** enantiomer are predicted to interact with the polymer C2 and C6 Ph groups via displaced–π (d–π) configurations. The MD-predicted NH···OH H-bond interaction is consistent with the IR shift of the polymer amide II band (Fig. 4 and Table 4). For the (+)-**1** enantiomer, these interactions occur synergistically in the polymer cavity since the methyl groups present in the solute structure do not disrupt these interactions. For the (−)-**1** enantiomer, the OH group is also predicted to interact with the polymer C3 NH group via a NH(C3)···OH((−)-**1**) H-bond. Three π–π interactions are predicted between the (−)-**1** enantiomer Ph groups and the polymer Ph groups. The d–π interaction is lower in energy than that of h or T configuration [25], consistent with the HPLC results. The difference between the strengths of the H-bond and the π–π interactions for the two enantiomers results from the steric hindrance from the fairly large $CH_3CHN(CH_3)_2$ group.

For compound **13**, the size of the sterically hindering group is smaller than that of compound **1** (Fig. 2). This allows for a better fit of both enantiomers in the polymer cavity, resulting in a NH(C3)···OH(**13**) H-bond. The small difference in the orientation of the Ph groups and the strength of the predicted H-bond for the two enantiomers of compound **13** are possibly due to the sterically hindering CH_3 group (Table 5), and result in a small enantioresolution. Compound **13** is the simplest compound used in this study for testing the commonly proposed three-point attachment (TPA) model [27,29,30]. For compound **1** with CDMPC, it appears that at least three synergistic and different sorbent–solute interactions, steric hindrance, H-bond, and π–π, result in a significant enantioresolution. Weakening of one of the interactions, via steric hindrance in compounds **13** and **2**, compared to compound **1**, results in decrease in the enantioresolutions.

For compound **3**, the higher retention factor compared to that of compound **1** can be attributed to an additional weak H-bond interaction between the polymer C6 C=O group and the solute NH group (Table 5) due to the absence of the two sterically hindering CH_3 groups compared to compound **1**. The small difference in

Table 5
Proposed sorbent–solute interactions in the CDMPC cavity

#	H-bond (H) interactions[a]	π–π Interactions		Inferred interactions[b]	*k*	*S*
	CSP gr···Solute gr.	CSP side chain	Type			
Benzyl alcohol	C3 NH···OH, or C6 C=O···HO	C2, C3, C6	h	1H, 3h	1.8	–
(1*S*,2*R*)-(+)-1	C3 NH···OH	C2, C6	d–π	1H, 2d–π	1.5	
(1*R*,2*S*)-(−)-1	C3 NH···OH	C3	T	1H, 2h, 1T	0.7	2.1
		C2, C6	h			
(1*S*,2*R*)-(+)-2	C3 NH···OH	C2, C6	d–π	1H, 2d–π	1.2	
(1*R*,2*S*)-(−)-2	C3 NH···OH	C3	T	1H, 2h, 1T	0.9	1.3
		C2, C6	h			
(1*S*,2*R*)-(+)-3	C3 NH···OH, C6 C=O···HN (w)	C2, C6	h	2H, 2h	2.4	1.2
(1*R*,2*S*)-(−)-3	C3 NH···OH, C6 C=O···HN (w)	C2, C3, C6	T	2H, 3T	2.0	
(1*S*,2*R*)-(+)-4	C3 NH···OH, or C3 NH···NH_2	C2, C6	h	1H, 2h, 1T (additional π–π interactions with neighboring rod)	3.1	
		C3	T			1.0
(1*R*,2*S*)-(−)-4	C3 NH···OH, or C3 NH···NH_2	C2, C6	h	1H, 2h, 1T (additional π–π interactions with neighboring rod)	3.1	
		C3	T			
5[e]	C3 NH···OH, or C3 NH···NH_2	–		1H	1.3	1.0
(1*R*)-(+)-6	C3 NH···OH	C2, C3, C6	h	1H, 3h	0.9	1.0
(1*S*)-(−)-6	C3 NH···OH	C2, C3, C6	h	1H, 3h	0.9	
(1*S*)-(+)-7	C3 NH···OH, C6 NH···NH_2(w)	C6	h	2H, 1h	3.2	1.1
(1*R*)-(−)-7	C3 NH···OH, C6 NH···NH_2(w)	C2	h	2H, 1h	3.0	
(2*S*)-(+)-8	C3 NH···NH_2, C6 NH···OH (w)	C6	h	2H, 1h	2.6	1.1
(2*R*)-(−)-8	C3 NH···NH_2, C6 NH···OH (w)	C2	h	2H, 1h	2.4	
9[c]	C3 NH···OH, or C3 NH···NH_2	–		1H	1.4	1.0
10[c]	C3 NH···OH, or C3 NH···OH	–		1H	0.9	1.0
(2*S*)-(+)-11	C3 NH···OH	C2	π	1H, 1π	0.9	1.3
(2*R*)-(−)-11	C3 NH···OH	C2, C6	h	1H, 2h	0.7	
(2*R*)-(+)-12	C3 NH···OH	C2, C6	h	1H, 2h	0.9	
(2*S*)-(−)-12	C3 NH···OH	C2	d–π	1H, 1d–π, 1h	0.9	1.0
		C6	h			
(1*R*)-(+)-13	C3 NH···OH	C2, C3, C6	h	1H, 3h	1.2	1.2
(1*S*)-(−)-13	C3 NH···OH	C2, C6	h	1H, 2h	1.0	

Based either on molecular mechanics or molecular dynamics.
Four different configurations between the sorbent and the solute phenyl (Ph) groups: (i) parallel staggered (π), (ii) parallel displaced (d–π), (iii) herringbone (h), and (iv) T-shaped (T).
[a] gr.: group.
[b] The interactions are inferred qualitatively. The strengths of H-bonding and π–π interactions for different solutes are different (see Table 4, IR results).
[c] Both enantiomers have the same interactions.

the strengths of the H-bonds and the π–π interactions, results in a reduced enantioresolution for compound **3**.

In order to test the presence of the proposed sorbent–solute H-bonding interactions, the retention factors of certain chiral solutes are also measured in pure 2-propanol mobile phase (results not shown here). The retention factors of these solutes are significantly lower compared to those in *n*-hexane/2-propanol (90/10, v/v) mobile phase, suggesting the weakening of the sorbent–solute H-bonds in the presence of pure 2-propanol. The enantioresolution observed for compound **1** is similar in both solvents. The enantioresolution observed for compound **1** in pure 2-propanol is due to the differences in the sorbent–solute π–π interactions (Table 5).

For compound (−)-**4**, the solute OH group forms an H-bond with the polymer C3 NH group. One of the solute Ph groups forms three π–π interactions with the polymer Ph groups. The second Ph group in the solute structure may not fit into the cavity and may form additional interactions with the neighboring polymer side chains from the same or adjacent polymer rods. These interactions may result in a high retention factor for the (−)-**4** enantiomer. The presence of one H-bonding group and one Ph group at each chiral center may confer this chemical structure some degree of symmetry, resulting in a similar number and types of interactions for (+)-**4** enantiomer in the polymer cavity, and hence no enantioresolution. The strengths of the H-bonding interactions of the solute OH and NH_2 groups with the polymer NH group are similar, as shown previously by the DFT calculations [6]. The results suggest that the presence of the four functional groups (one OH, one NH_2, and two Ph groups) does not guarantee an enantioresolution for a chiral solute if the compound functional groups are arranged with some symmetry in the polymer cavity without any steric hindrance, and the strengths of the interactions of the interacting functional groups are similar for the two enantiomers.

Compounds **5**, **9**, and **10** have two H-bonding functional groups and can interact with the polymer functional groups with either one strong or two weak H-bonding interactions (Table 5), resulting in lower retention factors and no enantioresolutions.

Compounds **6**, **11**, and **12** allow testing the effect of positioning a methylene group between the chiral center and one of the functional groups capable of H-bonding, Ph interaction, or steric hindrance. A methylene group allows various conformations because of the free rotations of its bonds. It was proposed previously that the two enantiomers can almost be superimposed in the same space when they approach the substrate binding sites from the same direction with a methylene group [26]. Both enantiomers of compound **6** (having a methylene group located between the chiral center and a sterically hindering CH_3 group), and compound

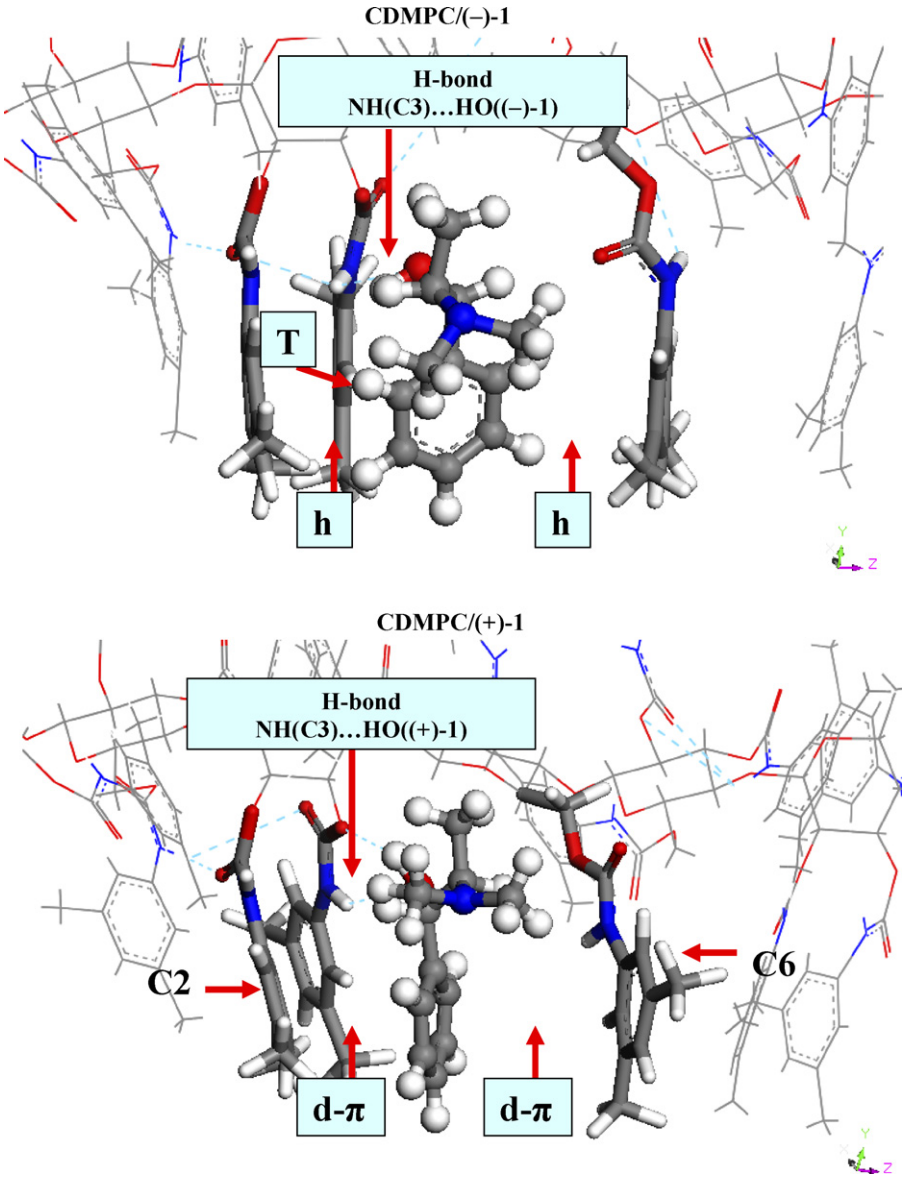

Fig. 6. Energy minimized structures of CDMPC complexes with (a) (−)-**1** enantiomer, and (b) (+)-**1** enantiomer. The dotted lines indicate H-bonds. The d–π, T, and h indicate parallel displaced, T-shaped, and herringbone π–π interactions, respectively.

12 (having a methylene group located between the chiral center and an H-bonding OH group) form similar number and type (H-bonding and π–π) interactions, resulting in no enantioresolution. On the other hand, even though compound **11** has a methylene group between the chiral center and a Ph group, the two enantiomers cannot be superimposed because of the bulky Ph group, resulting in limited enantioresolution.

Compared to compound **3**, compounds **7** and **8** do not have the CH_3 steric hindering group resulting in the loss of one chiral center. In these two compounds, a methylene group is located between the chiral center carrying one H-bonding group, and one Ph group and an H-bonding group. This geometry results in two H-bonds (one strong and one weak) and one π–π interaction for both enantiomers, resulting in significantly higher retention factors for both enantiomer pairs of compounds **7** and **8**. The two H-bonds formed for each enantiomer are similar, and the difference between the strengths of the π–π interactions is small, resulting in a small enantioresolution. The retention factor of compound **8** is slightly lower than that of compound **7** and their IR shifts are smaller (Table 4), possibly due to some differences in the strengths of the H-bonding interactions in these two compounds. The presence of a methylene group and the loss of a chiral center appear to reduce the enantioresolution.

3.4. Summary of the results

For CDMPC, a minimum of three synergistic and different interactions is required for chiral discrimination to arise for any chiral compound. The following qualitative trends are observed:

(a) A significant enantioresolution can result from steric hindrance, one H-bond, and π–π interactions (compound **1**).
(b) A small enantioresolution can result either from weak steric hindrance, H-bond, and π–π interactions (compounds **2**, and **13**) or from two H-bonds (one strong and one weak) and π–π interactions without any steric hindrance (compound **3**).
(c) No enantioresolution can result either from three or four similar interactions (H-bonding and π–π without any steric hindrance)

if there are symmetries in the compound functional groups (compound **4**) or if there are only one or two interactions (compounds **5**, **9**, and **10**).

(d) A methylene group between the chiral center and one of the functional groups can result in a small or negligible enantioresolution (compounds **6**, **7**, **8**, **11**, and **12**).

Quantitative predictions of enantioresolutions and retention factors would require considering all the discriminating and non-discriminating polymer cavities of varying sizes, substantial configurational sorbent–solute sampling, and solvent effects, and are not considered in this study. The TPA model is commonly cited for explaining the chromatographic separations [36–39]. This study and our previous studies [5,6] substantiate the validity of this model for the chiral solutes with CDMPC.

4. Conclusions

The HPLC retention factors and enantioresolutions of the enantiomer pairs of 13 structurally similar chiral solutes on the cellulose tris(3,5-dimethylphenylcarbamate) (CDMPC) chiral stationary phase, with 90/10 (v/v) *n*-hexane/2-propanol solvent at 298 K, are obtained. Of these chiral compounds, only methyl ephedrine (MEph) shows a significant enantioresolution. Variations in the number, the type of the interactions (H-bonding, π–π, and steric), and the spatial arrangements of the functional groups result in significantly different retention factors and enantioresolutions. The retention factors of 6 structurally similar simple non-chiral solutes are also studied for comparison, to help understand the nature of the sorbent–solute interactions. Upon adsorption of each solute, the IR spectra of the polymer amide groups change significantly, indicating H-bonding interactions and are used to identify the potential polymer binding sites. The MD-predicted structure of a 9-mer (3 unit cells) polymer chain is used to identify the potential cavities which can interact with the solutes. One cavity with three asymmetrically distributed polymer side chains was identified, and was used to study the polymer–solute H-bonding, π–π, and steric interactions. The MD-predicted binding sites in this cavity are consistent with the IR results, and can account qualitatively for the HPLC enantioresolution results. The inferences are consistent with the three-point attachment model. For the CDMPC polymer and the solutes tested, at least three different synergistic interactions, which can be steric hindrance, H-bond, or π–π, are needed to have a significant enantioresolution.

Acknowledgments

This research was supported in part by an NSF grant, CTS-0625189. We thank Dr. Geoffery Cox from Chiral Technologies (West Chester, PA, USA) for helpful advice and for supplying the Chiralcel OD silica beads and columns. We thank Dr. Chim Chin (School of Chemical Engineering, Purdue University) for his help and advice in chromatography experiments. We thank Dr. Srinivas Janaswamy (Department of Food Sciences, Purdue University, USA), for help in generating the polymer helical structure. We thank Prof. Igal Szleifer (Chemistry Department, Northwestern University, USA) and Dr. Marcelo Carignano (Department of Chemistry, Purdue University, USA), for their advice in MD calculations.

References

[1] C. Yamamoto, Y. Okamoto, Bull. Chem. Soc. Jpn. 77 (2004) 227.
[2] Y. Okamoto, Y. Kaida, J. Chromatogr. A 666 (1994) 403.
[3] H. Steinmeier, P. Zugenmaier, Carbohydr. Res. 164 (1987) 97.
[4] E. Yashima, C. Yamamoto, Y. Okamoto, J. Am. Chem. Soc. 118 (1996) 4036.
[5] R.B. Kasat, N.H.L. Wang, E.I. Franses, Biomacromolecules 8 (2007) 1676.
[6] R.B. Kasat, N.H.L. Wang, E.I. Franses, J. Chromatogr. A 1190 (2008) 110.
[7] M.L. Calabro, D. Raneri, S. Tommasini, R. Ficarra, S. Alcaro, A. Gallelli, N. Micale, M. Zappala, P. Ficarra, J. Chromatogr. B 838 (2006) 56.
[8] P.M. Cerqueira, V.B. Boralli, E.B. Coelho, N.P. Lopes, L.F.L. Guimaraes, P.S. Bonato, V.L. Lanchote, J. Chromatogr. B 783 (2003) 433.
[9] Y. Okamoto, E. Yashima, Angew. Chem., Int. Ed. 37 (1998) 1021.
[10] U. Selditz, S. Copinga, J.P. Franke, H. Wikstrom, R.A. deZeeuw, Chirality 8 (1996) 574.
[11] H.Y. Aboul-Enein, L.I. Abou-Basha, S.A. Bakr, Chirality 8 (1996) 153.
[12] S. Svensson, J. Vessman, A. Karlsson, J. Chromatogr. A 839 (1999) 23.
[13] Y. Fukui, A. Ichida, T. Shibata, K. Mori, J. Chromatogr. 515 (1990) 85.
[14] B. Chankvetadze, C. Yamamoto, Y. Okamoto, J. Chromatogr. A 922 (2001) 127.
[15] C. Yamamoto, E. Yashima, Y. Okamoto, Bull. Chem. Soc. Jpn. 72 (1999) 1815.
[16] Y. Okamoto, M. Kawashima, K. Hatada, J. Chromatogr. 363 (1986) 173.
[17] Y. Okamoto, K. Hatano, R. Aburatani, K. Hatada, Chem. Lett. issue 5 (1989) 715.
[18] E. Yashima, M. Yamada, C. Yamamoto, M. Nakashima, Y. Okamoto, Enantiomer 2 (1997) 225.
[19] T. O'Brien, L. Crocker, R. Thompson, K. Thompson, P.H. Toma, D.A. Conlon, B. Feibush, C. Moeder, G. Bicker, N. Grinberg, Anal. Chem. 69 (1997) 1999.
[20] B. Chankvetadze, E. Yashima, Y. Okamoto, J. Chromatogr. A 670 (1994) 39.
[21] Discover, 3.0 ed., Accelrys Inc., San Diego, California, 2003.
[22] P. Dauberosguthorpe, V.A. Roberts, D.J. Osguthorpe, J. Wolff, M. Genest, A.T. Hagler, Proteins: Struct. Funct. Genet. 4 (1988) 31.
[23] R.B. Kasat, C.Y. Chin, K.T. Thomson, E.I. Franses, N.H.L. Wang, Adsorption 12 (2006) 405.
[24] R.B. Kasat, Y. Zvinevich, H.W. Hillhouse, K.T. Thomson, N.H.L. Wang, E.I. Franses, J. Phys. Chem. B 110 (2006) 14114.
[25] S. Sun, E.R. Bernstein, J. Phys. Chem. 100 (1996) 13348.
[26] R. Bentley, Arch. Biochem. Biophys. 414 (2003) 1.
[27] V.A. Davankov, Chirality 9 (1997) 99.
[28] V. Sundaresan, R. Abrol, Protein Sci. 11 (2002) 1330.
[29] L.H. Easson, E. Stedman, Biochem. J. 27 (1933) 1257.
[30] A.G. Ogston, Nature 162 (1948) 963.
[31] L.J. Bellamy, The Infra-red Spectra of Complex Molecules, Wiley, New York, 1975.
[32] N.B. Colthup, L.H. Daly, S.E. Wiberley, Introduction to Infrared and Raman spectroscopy, Academic Press, Boston, 1990.
[33] S. Scheiner, Hydrogen Bonding: A Theoretical Perspective, Oxford University Press, New York, 1997.
[34] E.A. Meyer, R.K. Castellano, F. Diederich, Angew. Chem., Int. Ed. 42 (2003) 1210.
[35] B. Mey, H. Paulus, E. Lamparter, G. Blaschke, Chirality 11 (1999) 772.
[36] C.E. Dalgliesh, J. Chem. Soc. Oct. (1952) 3940.
[37] V.A. Davankov, A.A. Kurganov, Chromatographia 17 (1983) 686.
[38] W.H. Pirkle, C.J. Welch, M.H. Hyun, J. Org. Chem. 48 (1983) 5022.
[39] S. Vidyasankar, M. Ru, F.H. Arnold, J. Chromatogr. A 775 (1997) 51.